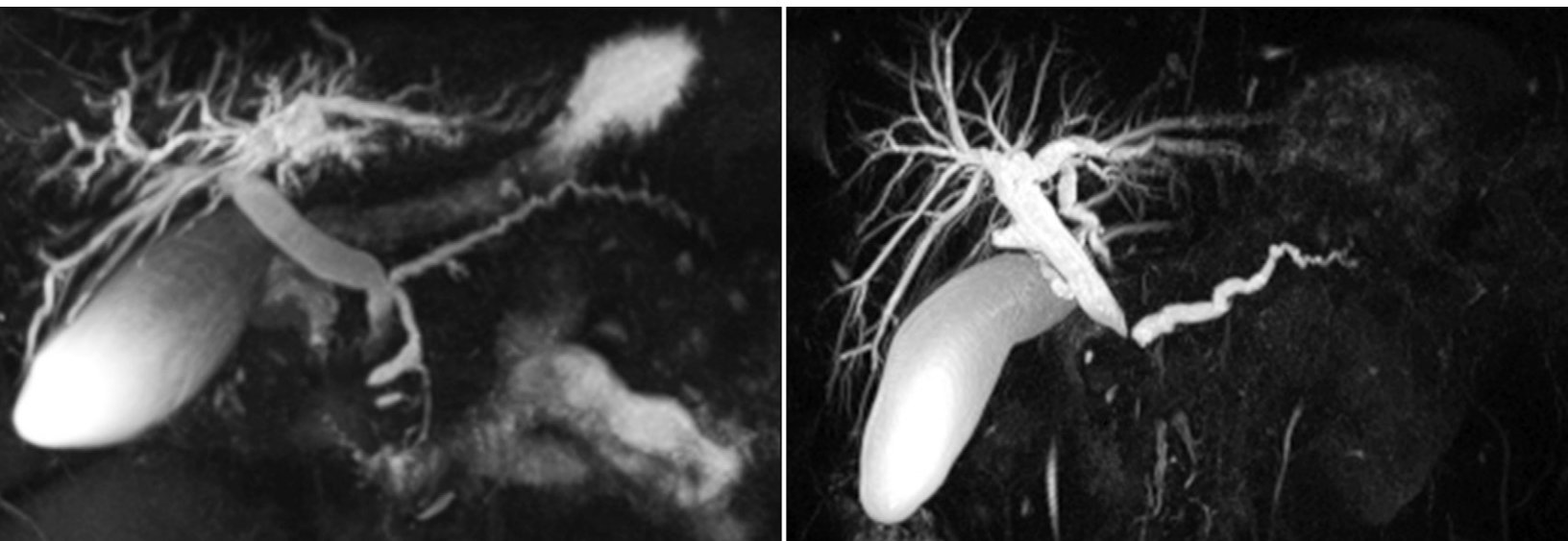


Pancreatic Cancer and Its Mimics

Frank H. Miller, MD • Camila Lopes Vendrami, MD • Nancy A. Hammond, MD • Pardeep K. Mittal, MD
Paul Nikolaidis, MD • Anugayathri Jawahar, MD

Author affiliations, funding, and conflicts of interest are listed at the end of [this article](#).
See the invited commentary by [Zins](#) in this issue.



Pancreatic ductal adenocarcinoma (PDAC) is the most common primary pancreatic malignancy, ranking fourth in cancer-related mortality in the United States. Typically, PDAC appears on images as a hypovascular mass with upstream pancreatic duct dilatation and abrupt duct cutoff, distal pancreatic atrophy, and vascular encasement, with metastatic involvement including lymphadenopathy. However, atypical manifestations that may limit detection of the underlying PDAC may also occur. Atypical PDAC features include findings related to associated conditions such as acute or chronic pancreatitis, a mass that is isointense to the parenchyma, multiplicity, diffuse tumor infiltration, associated calcifications, and cystic components. Several neoplastic and inflammatory conditions can mimic PDAC, such as paraduodenal “groove” pancreatitis, autoimmune pancreatitis, focal acute and chronic pancreatitis, neuroendocrine tumors, solid pseudopapillary neoplasms, metastases, and lymphoma. Differentiation of these conditions from PDAC can be challenging due to overlapping CT and MRI features; however, certain findings can help in differentiation. Diffusion-weighted MRI can be helpful but also can be nonspecific. Accurate diagnosis is pivotal for guiding therapeutic planning and potential outcomes in PDAC and avoiding biopsy or surgical treatment of some of these mimics. Biopsy may still be required for diagnosis in some cases. The authors describe the typical and atypical imaging findings of PDAC and features that may help to differentiate PDAC from its mimics.

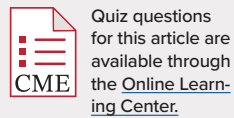
©RSNA, 2023 • radiographics.rsna.org

Introduction

Pancreatic ductal adenocarcinoma (PDAC) is the most common primary neoplasm of the pancreas, accounting for 90% of all pancreatic cancers (1). In the United States, PDAC accounts for 3.2% of all new cancer cases and 8% of all cancer deaths, ranking fourth in cancer-related mortality (2). Although surgery is the only curative treatment, at diagnosis an estimated 10%–20% of patients have resectable tumors, 30%–40% have borderline resectable or locally advanced or unresectable neoplasms, and 50%–60% have metastatic or systemic disease (3). PDAC is frequently detected late because of its nonspecific

clinical presentation and lack of specific tumor markers and the limitations in imaging early-stage neoplasms, resulting in a poor prognosis (2,3). The overall 5-year survival rate of PDAC is 10%, with higher 5-year survival rates of 41.6% in stage I or localized disease and extremely poor survival rates for stage IV metastatic disease (3%) (1).

Radiologists play a critical role in the diagnosis of PDAC. Typically, PDAC appears as an ill-defined hypovascular mass at CT or MRI. Atypical imaging features can also be seen. The appearance of PDAC can overlap with those of a wide range of abnormalities, including inflammatory conditions



Supplemental Material

TEACHING POINTS

- The indirect signs of isoattenuating PDACs that provide clues to the diagnosis include upstream parenchymal atrophy, focal contour abnormality, mass effect, interrupted duct sign, and perivascular tumor infiltration.
- Mass-forming chronic pancreatitis is uncommon but mimics PDAC. PDAC and mass-forming chronic pancreatitis can have similar CT and MRI findings including a hypoattenuating or hypointense hypoenhancing mass, with the double duct sign, ductal strictures, and peripancreatic infiltration. MRI findings of mass-forming chronic pancreatitis from fibrosis can be similar to those of PDAC and include decreased signal intensity of the normally hyperintense pancreas at fat-suppressed T1-weighted MRI, decreased and delayed enhancement after administration of intravenous contrast material, and restricted diffusion.
- Imaging features of PDP and paraduodenal cancer may overlap because of the significant fibrous component of both lesions, which demonstrates delayed enhancement. PDP has been reported to represent 28% of pseudotumoral pancreatitis, where patients underwent pancreatoduodenectomy for preoperative diagnosis of cancer but their disease was benign at histopathologic examination. PDP with resultant stricture of the duodenum (without cysts) can pose an imaging challenge. There are certain imaging features that can help to differentiate PDP from PDAC. Focal thickening of the second portion of the duodenum, cystic changes in the duodenal wall or pancreaticoduodenal groove, and abnormal enhancement of the second portion of the duodenum favor PDP over cancer.
- AIP may be difficult to distinguish from PDAC at imaging because both can appear as a focal or infiltrative mass. Features favoring AIP include homogeneous enhancement during the portal venous phase, a hypointense capsule-like rim, extrapancreatic manifestations, the absence of pancreatic atrophy, and excellent response to steroid treatment.
- Small neuroendocrine tumors can cause ductal dilatation and obstruction and upstream pancreatic atrophy secondary to secretion of serotonin and other metabolites, causing fibrotic narrowing of the main pancreatic duct. Marked pancreatic duct dilatation and stenosis and pancreatic atrophy out of proportion to an underlying hypervascular mass suggest a serotonin-producing PanNET.

(acute and chronic mass-forming pancreatitis, autoimmune pancreatitis, and paraduodenal pancreatitis), pancreatic neuroendocrine tumors, solid pseudopapillary neoplasms, and metastases. Distinguishing these abnormalities and PDAC can be challenging; however, certain features may help in differentiating them. Nevertheless, biopsy may still be required in some cases.

In this article, we describe the typical and atypical appearances of PDAC and features that help differentiate it from its mimics, with the aim of improving management and outcomes.

Imaging Techniques

Recommended CT and MRI protocols based on consensus guidelines for pancreatic imaging have been described, but a

detailed discussion of these protocols is beyond the scope of this article. The CT pancreatic protocol includes dual-phase multidetector CT performed with a section thickness of 1–3 mm, with images acquired during the pancreatic (40–50 seconds after injection of a contrast material bolus) and portal venous (65–70 seconds) phases. Optional acquisition during the delayed phase (240 seconds) has been recommended for some masses that are isoattenuating to the parenchyma during the parenchymal phase (4). The recommended contrast material has a high iodine concentration at an injection rate of 3–5 mL per second (5,6). The pancreatic parenchymal phase is slightly delayed when compared with a traditional arterial phase. The split-bolus protocol for pancreatic imaging can be helpful, with 100 mL of intravenous contrast material injected initially and a second bolus of 40 mL injected 35 seconds later at a rate of 4–5 mL per second. The scan is triggered by bolus tracking software at 15 seconds after the aortic enhancement reaches 280 HU to acquire simultaneous pancreatic and portal venous phase images. This protocol improves tumor visualization and reduces the radiation dose by 43% compared with that of the standard dual-phase protocol (5,7). Other variations include dose adjustments based on patient body weight, bolus timing, and injection rates. Although many studies in the 1990s and early 2000s showed that CT is more sensitive and accurate than MRI (8), studies from the early to mid 2010s (9,10) have shown that MRI is comparable and, in certain situations, superior to CT, for example, to detect isoattenuating PDAC where MRI with diffusion-weighted imaging (DWI) can be advantageous.

Recommended MRI protocols for pancreatic imaging include coronal and axial T2-weighted single-shot fast spin-echo imaging; axial T1-weighted in-phase and opposed-phase gradient-echo imaging; axial T2-weighted fat-suppressed fast spin-echo imaging; axial DWI ($b = 50, 500, \text{ and } 1000 \text{ sec/mm}^2$); axial pre- and postcontrast three-dimensional T1-weighted fat-suppressed gradient-echo imaging during the arterial, portal venous, and delayed phases at a 3–5 minute delay; and coronal T2-weighted MR cholangiopancreatography (MRCP) (11,12). The in- and opposed-phase and subtraction images can be helpful to confirm focal fat when there is uncertainty on multidetector CT images of a mass (Fig S1).

Imaging Findings of PDAC

The typical appearance of PDAC at cross-sectional imaging is a hypoenhancing infiltrative mass, relative to the remainder of the pancreas on late arterial (pancreatic) and portal venous phase images, with delayed enhancement on later phase images because of decreased vascularity and desmoplastic stroma (13). Upstream pancreatic duct dilatation and atrophy are common (Fig 1). PDAC appears hypointense on unenhanced fat-suppressed T1-weighted MR images and is best seen on early parenchymal phase images, with progressive enhancement on delayed phase images and mild hyperintensity on T2-weighted MR images. A dilated pancreatic duct and common bile duct (ie, the “double duct” sign) suggest an underlying pancreatic head mass, even if it is not visualized (4,11). Lesions involving the pancreatic tail manifest late with metastases and are often infiltrative, lacking pancreatic duct

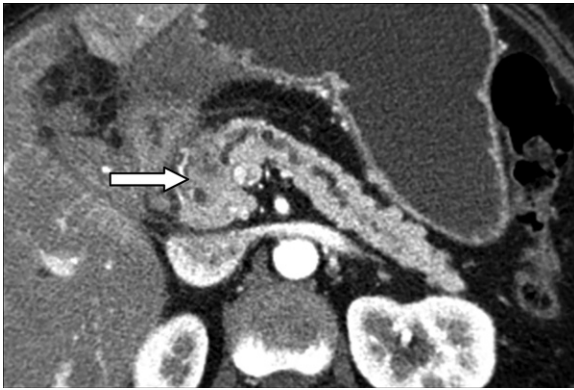


Figure 1. Typical CT appearance of PDAC in a 58-year-old woman. Axial contrast-enhanced CT image shows a hypo-enhancing mass in the pancreatic head (arrow) with an upstream dilated pancreatic duct.



Figure 2. Unsuspected PDAC in the background of acute pancreatitis in a 63-year-old man (same patient as in Fig 11). Axial contrast-enhanced CT image shows a dilated main pancreatic duct (long straight arrow) with a cutoff in the pancreatic genu and an isoattenuating mass with mild contour deformity (curved arrow). The patient had acute pancreatitis, including enlargement of the pancreatic tail and peripancreatic fat stranding (short arrow).

dilatation (Fig S2). DWI may allow early detection of PDAC and can help to detect hepatic metastases, peritoneal implants, and lymph nodes. Secondary findings are essential to identify and include a contour abnormality, abrupt termination of the biliary or pancreatic duct (with or without upstream dilatation), a high pancreatic duct to parenchyma ratio, and pancreatic atrophy upstream from the mass. Vascular encasement (Fig S3), peritoneal implants, and liver metastases in a patient with a pancreatic mass should suggest pancreatic cancer over other diagnoses.

The abrupt pancreatic duct cutoff sign is associated with a high incidence of PDAC (Fig 2). Gangi et al (14) studied patients with pancreatic cancer who were asymptomatic before the diagnosis of cancer and found features suspicious for cancer in 50% of patients 2–18 months before diagnosis, including pancreatic duct dilatation with a cutoff. Johnston et al (2) showed that 58% of patients identified with duct cutoff received a diagnosis of malignancy, 62% of whom had PDAC (2). However, this sign is not diagnostic of PDAC because it can also be seen in chronic pancreatitis including “masslike” pancreatitis or intraductal stones (Fig 3). Nevertheless, abrupt duct cutoff without a stone or underlying cause on CT images warrants expedited workup with MRI or endoscopic US and potentially biopsy to exclude malignancy (2). Toshima et al (15), in a case control series of 206 patients, reported that 53.4% of patients with clinical stage I PDAC had focal pancreatic changes on CT images acquired at least 1 year before diagnosis, most commonly focal atrophy (37.9%), faint parenchymal enhancement (26.2%), and focal main pancreatic duct change (13.6%) seen 4.6, 3.3, and 1.1 years before diagnosis, respectively. DWI can be helpful to distinguish PDAC from the background parenchyma, especially for detection of small non-contour-deforming masses (2,16,17). Unfortunately, DWI, similar to anatomic imaging, is not specific for PDAC. PDACs often have dense cellularity or extracellular fibrosis, which is associated with significantly lower apparent diffusion coefficients, and as result, DWI can be helpful in detection of a mass that may not be seen on images from all sequences; however, DWI has limitations because not all cancers are identifiable with only DWI. Other MRI sequences, especially conventional T1-weighted fat-suppressed and early

contrast-enhanced images, should routinely be evaluated in conjunction with DWI. In addition, although DWI is helpful in detection, it has the same limitations as conventional imaging in distinguishing mass-forming chronic pancreatitis and other entities from PDAC because they are associated with fibrosis and inflammatory changes (16,18,19).

Although some studies (16–18) have shown that DWI can be helpful in distinguishing poorly differentiated PDACs with lower apparent diffusion coefficients from well- or moderately differentiated PDACs, others have shown that apparent diffusion coefficients are not helpful because of overlap likely related to variability in the amount of fibrosis, necrosis, and cellular density within tumors. DWI is especially helpful in detection of lymph node and peritoneal implants and detection and characterization of liver metastases, which may preclude surgery. In a multicenter trial (19), the use of MRI with DWI in comparison to the use of CT for detection of liver metastases changed treatment and surgery plans in 10% of patients with potentially resectable PDACs.

Atypical Features of PDAC

Although most PDACs show classic imaging features, patients can present with atypical features that radiologists must recognize to avoid misdiagnosis. These atypical findings can relate to associated conditions such as acute or chronic pancreatitis and may limit detection of an underlying PDAC. Other atypical features include a mass that is isoattenuating to the parenchyma, multiplicity, diffuse tumor infiltration, associated calcifications, and cystic components.

Isoattenuating masses relative to the surrounding normal parenchyma (within 10 HU) on pancreatic and portal venous phase images are challenging to identify, and they account for a reported incidence of 5.4%–14% of PDACs (Fig 2) (4,20). These tumors are usually smaller than the typical hypoattenuating PDACs and are indistinguishable from the surrounding parenchyma (21). Histologically, these are often well-differentiated tumors with low cellularity, and patients who have

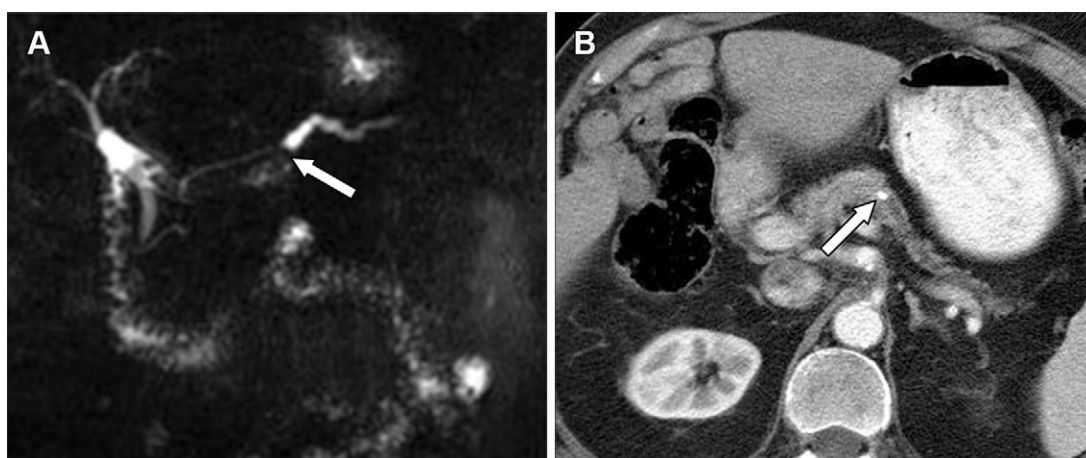


Figure 3. Abrupt termination of the duct because of a stone in a 45-year-old man with chronic pancreatitis. (A) Coronal rapid acquisition with relaxation enhancement MRCP image shows a dilated pancreatic duct with abrupt termination of the duct in the pancreatic body (arrow). No associated mass or stone is visible. (B) Axial contrast-enhanced CT image shows a calcified stone (arrow) in the pancreatic duct, instead of a mass at the site of ductal termination as seen on the MR image.



Figure 4. PDAC in a 66-year-old woman with a history of several liver lesions seen at US (not shown) concerning for metastatic disease. Axial contrast-enhanced CT image shows an ill-defined, solid, low-attenuation mass measuring 4.6 cm in the pancreatic head, with the cystic component measuring 3.4 cm (long arrow). Clues to the diagnosis of PDAC include the heterogeneous lesion with an enhancing solid component (short arrow). The lack of a history or clinical findings of pancreatitis also should suggest PDAC.

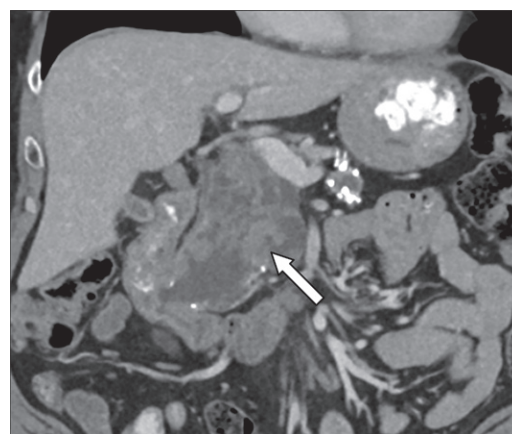


Figure 5. PDAC arising from an intraductal papillary mucinous neoplasm in the main duct in a 62-year-old man. Coronal contrast-enhanced CT image shows a large heterogeneous cystic mass in the pancreatic head measuring 9.6 cm, with solid components (arrow). Biopsy results showed moderately differentiated invasive PDAC.

them have been reported to have prolonged survival after surgery when compared with that of typical PDACs (22). The indirect signs of isoattenuating PDACs that provide clues to the diagnosis include upstream parenchymal atrophy, focal contour abnormality, mass effect, interrupted duct sign, and perivascular tumor infiltration (23,24). Secondary signs such as biliary and pancreatic duct dilatation are not seen in 14% of PDACs, especially those that are isoattenuating to the uncinate process and are present at an earlier stage compared with PDACs with secondary signs (25). Pancreatic tail tumors also are less likely to show pancreatic duct dilatation and instead show subtle changes in texture and loss of normal fatty lobulations that may indicate an underlying mass (26). Ishigami et al (4) recommend that for pancreatic masses that are isoattenuating during the pancreatic parenchymal phase (45 seconds), delayed phase images (240 seconds), on which they may appear slightly hyperattenuating to the parenchyma, should be obtained to increase sensitivity for PDAC. In addition, MRI and PET/CT may be useful in detecting 79.2% and 73.7% of isoattenuating PDACs, respectively (20). When a suspected mass is not visualized at either

CT or MRI, endoscopic US and biopsy should be considered for tissue diagnosis.

Other uncommon atypical findings of PDAC include cystic changes, calcifications, diffuse infiltration, and multifocal masses. PDAC may have intratumoral cystic features or may accompany peritumoral nonneoplastic cystic lesions in 7%–8% of patients (Fig 4). These cystic changes can relate to necrosis, an underlying cystic neoplasm, or associated retention cysts or pseudocysts (27). PDAC associated with upstream large pseudocysts in a patient with acute pancreatitis can obscure the primary solid tumor. The lesion may also appear solid and cystic when it represents PDAC arising from a branch duct or main duct intraductal papillary mucinous neoplasm (28). The cystic component may appear more tubular from main or branch duct involvement, which may help in the diagnosis (Fig 5). PDAC rarely has calcifications (1%–2%) (Fig 6) and when present mostly occurs within a background of chronic calcific pancreatitis. Other causes of calcifications in PDAC are pancreatic ductal obstruction by tumor and dystrophic calcifications (29). A solid pancreatic tumor with calcification, even if it is hypoattenuating, most likely represents



Figure 6. PDAC in a 68-year-old woman. Axial contrast-enhanced CT image shows an enlarged heterogeneous pancreatic head, suggesting the presence of an underlying tumor (long arrow) with intratumoral calcification (short arrow), a rare finding in PDAC.

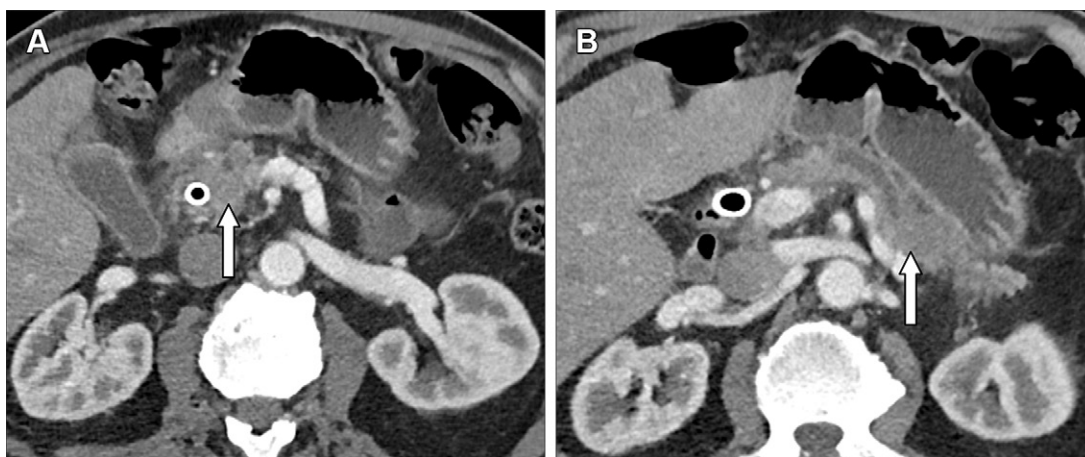


Figure 7. Synchronous PDAC in a 67-year-old man with a history of abdominal pain, fatty stools, and dark urine. (A) Axial contrast-enhanced CT image shows a hypo-enhancing mass in the pancreatic head (arrow), which is consistent with known PDAC, and a wall stent in the common bile duct. (B) Axial contrast-enhanced CT image shows an additional mass in the pancreatic tail from synchronous PDAC (arrow). After chemotherapy, the patient underwent pancreaticoduodenectomy, distal pancreatectomy, and splenectomy.

a neuroendocrine tumor and not PDAC. Diffuse tumor infiltration is seen in 1%–5% of PDACs and can imitate the imaging findings of an inflammatory process such as autoimmune pancreatitis, lymphoma, acinar cell carcinoma, a neuroendocrine tumor, and pancreatic metastasis (30). Multifocal masses from PDAC are uncommon (Fig 7) and more commonly seen in pancreatic metastases, secondary diffuse pancreatic lymphoma, or autoimmune pancreatitis (AIP). They may relate to contiguous tumors (23) and may be associated with main duct intraductal papillary mucinous neoplasms.

Mimics

Mass-forming Chronic Pancreatitis

Chronic pancreatitis is a result of repeated episodes of inflammation of the pancreas, leading to parenchymal fibrosis and glandular atrophy. Chronic pancreatitis causes irreversible permanent structural damage to the pancreas, resulting in impairment of both endocrine and exocrine functions (31). Mass-forming chronic pancreatitis is uncommon but mimics PDAC (Table 1) (32–35). PDAC and mass-forming chronic pancreatitis can have similar CT and MRI findings including a hypoattenuating or hypointense hypo-enhancing mass, with the double duct sign, ductal strictures, and peripancreatic infiltration. MRI findings of mass-forming chronic pancreatitis from fibrosis can be similar to those of PDAC and include decreased signal intensity of the normally hyperintense pancreas

at fat-suppressed T1-weighted MRI, decreased and delayed enhancement after administration of intravenous contrast material, and restricted diffusion (31,32,36,37). Distinguishing features that favor diagnosis of an inflammatory mass in chronic pancreatitis over PDAC are a smoothly tapering duct coursing through the mass called the “duct-penetrating sign” (96% specificity, 85% sensitivity, and 94% accuracy) (34) (Fig 8), branch duct dilatation from the traction effect of parenchymal fibrosis, irregularity of pancreatic ducts, pseudocysts, and diffuse parenchymal and intraductal calcifications (31,34,35). Endoscopic US-guided biopsy may be required to differentiate mass-forming chronic pancreatitis from pancreatic cancer (36).

Chronic pancreatitis and PDAC can be seen concomitantly. Chronic pancreatitis increases the risk of PDAC, and PDAC can result in upstream obstructive chronic pancreatitis (31). Patients with a diagnosis of chronic pancreatitis have a 16-fold increased risk of PDAC, especially in the first few years after receiving the diagnosis. This led authors of a meta-analysis (38) to suggest initial close follow-up of patients with chronic pancreatitis to avoid misclassifying cancer as chronic pancreatitis or missing a coexisting cancer. However, the current guidelines do not recommend routine follow-up, except in patients at high risk for cancer.

Focal Acute Pancreatitis

Focal acute pancreatitis can mimic PDAC and includes focal forms of interstitial edematous pancreatitis and necrotizing

Table 1: Differentiating Mass-forming Chronic Pancreatitis from PDAC

Feature	Mass-forming Chronic Pancreatitis	PDAC
Duct penetrating sign	Present	Absent
Branch duct status	Pancreatic branch duct dilation in the upstream pancreas	Obliterated branch ducts adjacent to malignancy (mass effect)
Double duct sign	Usually absent	Present
Abrupt duct cutoff sign	Absent	Abrupt duct cutoff sign common
Duct to parenchyma ratio	<0.34	>0.34
Duct dilatation	Mild dilatation	Marked upstream dilatation
Parenchymal atrophy	Mild	Present
Calcifications	Scattered parenchymal	Peripherally displaced
Vascular encasement	Absent	Present, especially of peripancreatic arteries
SMA to SMV ratio	<1.0	>1.0

Sources.—References 32–35.

Note.—SMA = superior mesenteric artery, SMV = superior mesenteric vein.

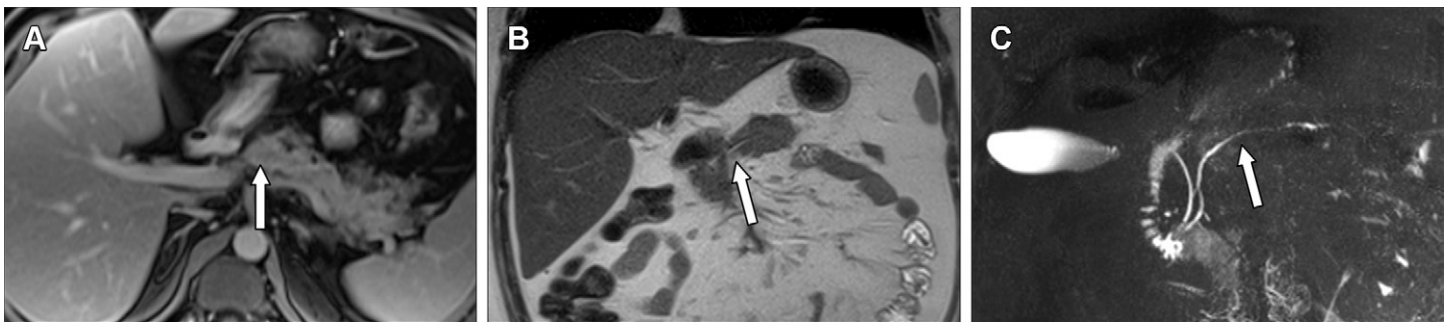


Figure 8. Chronic masslike pancreatitis in a 33-year-old man with a history of recurrent pancreatitis. (A) Axial contrast-enhanced T1-weighted fat-suppressed MR image shows prominent enhancing tissue involving the body of the pancreas that appears ill defined and masslike (arrow). (B, C) T2-weighted (B) and three-dimensional MRCP (C) images show the duct-penetrating sign, with a patent duct extending through the apparent mass (arrow), suggesting findings against cancer.

pancreatitis. Clinical parameters including an elevated lipase level and abdominal pain can often help distinguish focal acute pancreatitis from PDAC. Imaging findings of focal acute pancreatitis include enlargement of the pancreas, decreased and heterogeneous enhancement, and peripancreatic inflammation and fluid. Disconnected duct syndrome, which is associated with necrotizing pancreatitis, can be confused with PDAC because of its abrupt terminating duct and masslike appearance, especially when the history of necrotizing pancreatitis may not be known (39) (Fig 9).

The association of chronic pancreatitis and PDAC is well known and common. However, less well known but also important is that results of recent studies (40–42) have shown that 6.8%–13.8% of patients with acute pancreatitis have coexisting PDAC, particularly patients older than 40 years of age. Munigala et al (40) found that 10.7% of patients with PDAC had acute pancreatitis 2 years before diagnosis of PDAC and that diagnosis of PDAC was delayed by at least 2 months after an episode of acute pancreatitis in more than one-half of these patients (14,40). The association between PDAC and pancreatitis is thought to relate to ductal obstruction caused by PDAC, resulting in acute pancreatitis clinically and masking the PDAC (40). Hence, a high index of suspicion for PDAC is important, and further evaluation for underlying PDAC is

recommended in patients for whom an underlying cause for acute pancreatitis is unknown, especially in patients more than 40 years old (Fig 10) (40).

Identification on imaging studies of an underlying mass suggests PDAC in patients with acute pancreatitis. The findings of an abrupt terminating duct sign in patients with pancreatitis and the lack of intraductal stones on CT or US images should increase suspicion for an underlying mass and may warrant the use of MRI or endoscopic US (Fig 11). Other features that increase suspicion for PDAC include vascular encasement (Fig S3), which is less commonly seen in acute pancreatitis. If there is uncertainty for underlying PDAC on CT images, short-term follow-up imaging is recommended with endoscopic US and/or MRI. For definitive diagnosis, biopsy may be required, although it is often avoided during the acute inflammatory phase.

Paraduodenal Pancreatitis and Paraduodenal Cancer

Paraduodenal pancreatitis (PDP), also referred to as “groove” pancreatitis, is a rare form of focal chronic pancreatitis that results from repeated episodes of pancreatitis or acute exacerbation of chronic pancreatitis and may mimic PDAC. The pathogenesis of PDP is unclear, but it is thought to be multifactorial. The prototypical patient is a middle-aged man (40–50

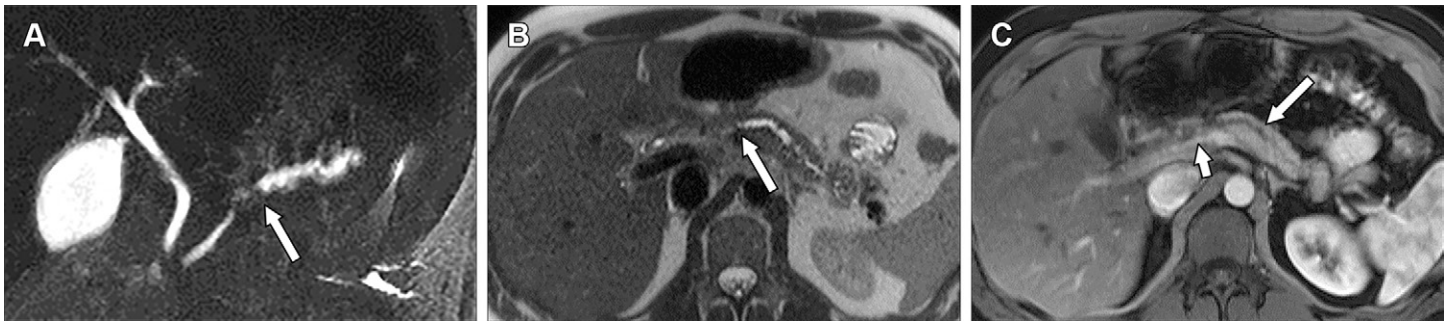


Figure 9. Disconnected duct mimicking a mass in a 45-year-old man with a history of necrotizing pancreatitis. (A, B) MRCP (A) and T2-weighted MR (B) images show a dilated duct (arrow) with an abrupt termination suggestive of an underlying mass (PDAC) from a disconnected duct associated with pancreatitis. (C) Axial early phase T1-weighted fat-suppressed MR image shows a dilated pancreatic duct (long arrow) and inflammatory changes mimicking a mass (short arrow).

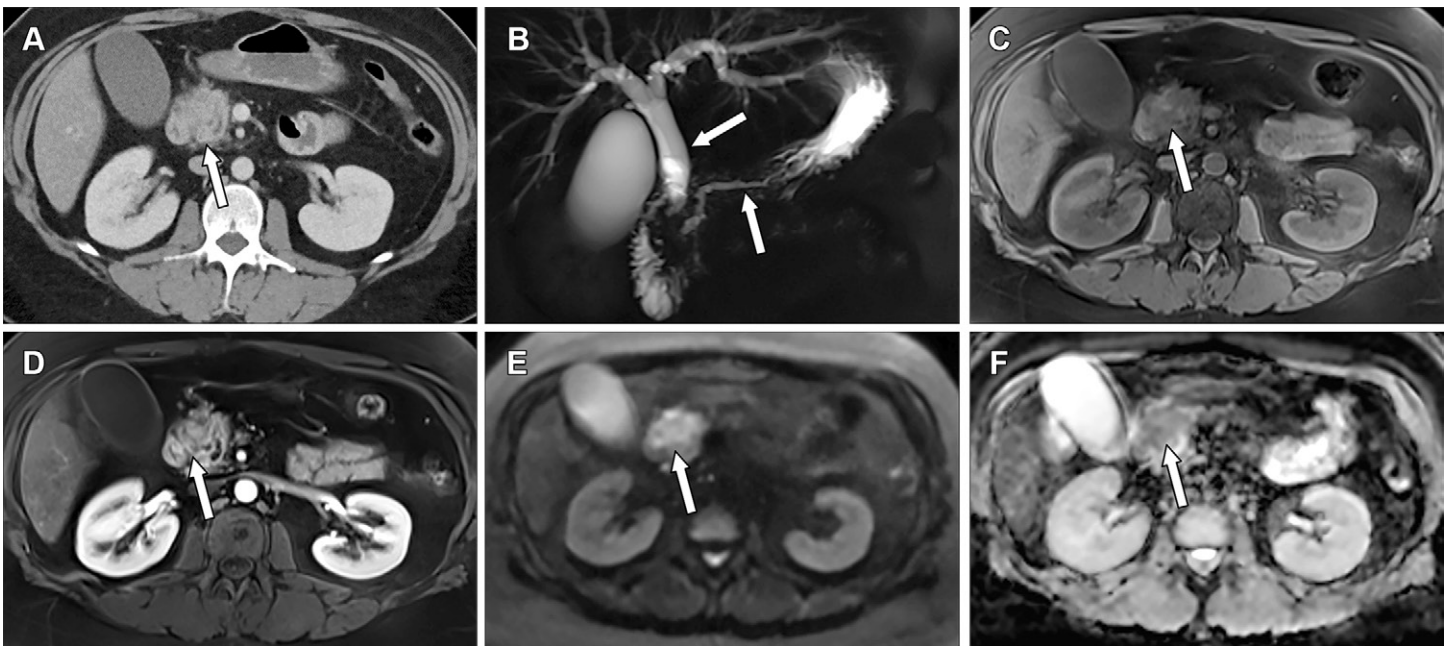


Figure 10. Infiltrating PDAC in an background of acute pancreatitis in a 42-year-old woman with a history of an elevated lipase level and hyperbilirubinemia. (A) Axial contrast-enhanced CT image shows a masslike area in the pancreatic head (arrow) with mild fat stranding that was believed to be acute pancreatitis. Because of clinical concern for an underlying mass, MRI was performed. (B) MRCP image shows the double duct sign, with pancreatic duct dilatation and associated common and intrahepatic duct dilatation (arrows). (C) Axial unenhanced T1-weighted fat-suppressed MR image shows hypointensity (arrow) relative to the normal high-signal-intensity pancreas. (D) Early contrast-enhanced T1-weighted fat-suppressed MR image shows a heterogeneous enhancing area in the pancreatic head (arrow), with associated fat stranding, suggestive of inflammation. (E, F) Axial diffusion-weighted MR image ($b = 1000 \text{ sec/mm}^2$) (E) shows signal hyperintensity (arrow), and axial apparent diffusion coefficient map (F) shows low signal intensity from restricted diffusion (arrow). The appearance, however, is nonspecific and can be seen in inflammatory masses and cancer. Endoscopic US-guided biopsy results showed infiltrating moderately differentiated PDAC.

years old), with a history of overconsumption of alcohol. The true incidence of PDP is unknown, but the reported range is 2.7%–24.4% of patients who underwent pancreatic resection for chronic pancreatitis (43).

PDP involves the pancreaticoduodenal groove, a potential space among the duodenum, pancreatic head, and the distal common bile duct. Two forms of PDP exist: the pure form, which affects only the pancreaticoduodenal groove and spares the pancreatic head, and the segmental form, which is centered in the groove but extends medially to involve the head (36,44,45). On CT images, the classic imaging finding is delayed enhancing soft tissue in the groove. Small cysts may be seen along the medial wall of the duodenum. On MR images, the pure form of PDP appears as a sheetlike mass between the pancreatic head and the duodenal “C” loop. This fibrotic

mass is hypointense on T1-weighted MR images and shows variable signal intensity on T2-weighted MR images, depending on the time since onset (Fig 12). In the subacute phase, T2 hyperintensity occurs from edema, but as it progresses to fibrosis, it becomes T2 hypointense. Because of its fibrous nature, dynamic contrast-enhanced MR images demonstrate delayed enhancement (36). Medial duodenal wall thickening is noted in both the pure and segmental forms of PDP. Hyperintense T2-weighted cysts can develop in the duodenal wall and the pancreaticoduodenal groove (Fig 13), mimicking pancreatic pseudocysts, duplication cysts, and cystic tumors (46).

In the segmental form, masslike enlargement of the pancreatic head obscures the groove and demonstrates T1 hypointensity, mimicking PDAC (36,44). In both forms of PDP, the common bile duct can appear narrowed, with

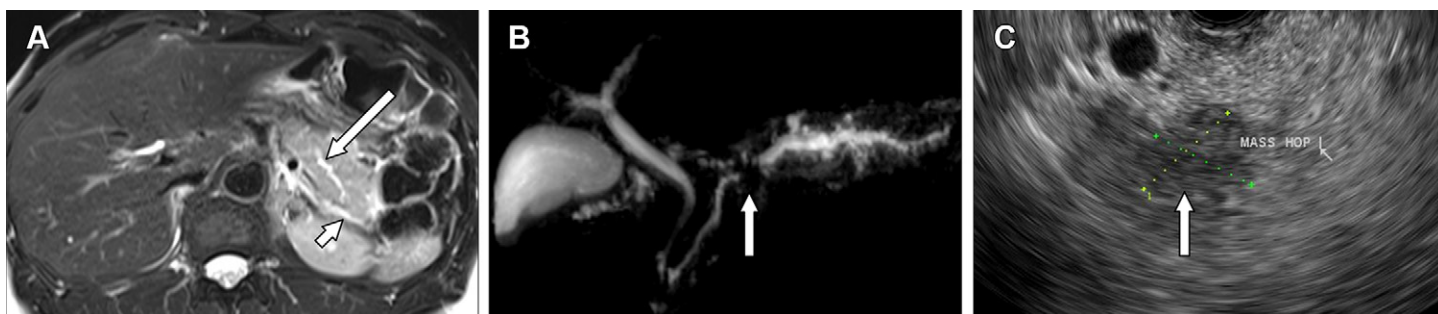


Figure 11. Unsuspected PDAC in a background of acute pancreatitis in a 63-year-old man (same patient as in Fig 2). Because acute pancreatitis of unknown cause was seen at a CT examination (Fig 2), an MRI examination was performed. (A) Axial T2-weighted fat-suppressed MR image shows a dilated duct (long arrow) and findings of pancreatitis involving the tail (short arrow). (B) MRCP image shows an abrupt terminating duct sign (arrow). The abrupt termination of the duct raised concern for an underlying mass, prompting endoscopic US. (C) Endoscopic US image shows a mass (arrow) as the cause of ductal dilatation that was biopsy-proven PDAC.

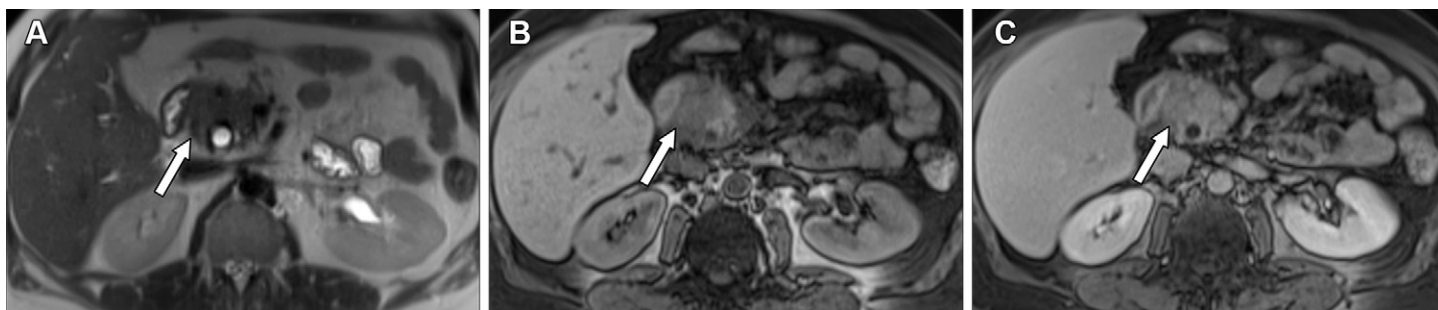


Figure 12. Solid pattern of PDP in a 55-year-old man with a history of alcohol overuse and upper abdominal pain. (A) Axial T2-weighted MR image shows a hypointense lesion (arrow) in the paraduodenal groove suggestive of fibrosis. (B) Axial T1-weighted fat-suppressed MR image shows a hypointense lesion (arrow) in the groove. (C) Axial contrast-enhanced T1-weighted fat-suppressed MR image shows early hypoenhancement (arrow), with more delayed enhancement present on images from delayed sequences (not shown). Wall thickening in the second portion of the duodenum enhanced after contrast material administration. The lack of cysts makes it more difficult to distinguish it from paraduodenal cancer, but the enhancement pattern is more characteristic of PDP.

smooth tapering to the ampulla and without shouldering or irregular abrupt margins or complete obstruction in distinction to paraduodenal (groove) adenocarcinoma (36,44,45). Narrowing of the pancreatic duct can also occur in a smooth and gradual fashion toward the pancreatic head. The distance between the ampulla and the duodenal lumen is typically widened in patients with PDP (36,44,45).

Imaging features of PDP and paraduodenal cancer may overlap because of the significant fibrous component of both lesions, which demonstrates delayed enhancement (Fig 14) (Table 2) (36,44,45). PDP has been reported to represent 28% of pseudotumoral pancreatitis, where patients underwent pancreatoduodenectomy for preoperative diagnosis of cancer but their disease was benign at histopathologic examination (47). PDP with resultant stricture of the duodenum (without cysts) can pose an imaging challenge (Fig 15). There are certain imaging features that can help to differentiate PDP from PDAC. Focal thickening of the second portion of the duodenum, cystic changes in the duodenal wall or pancreaticoduodenal groove, and abnormal enhancement of the second portion of the duodenum favor PDP over cancer (45). Distinguishing PDP from cancer can be difficult with the solid variant when there are no cysts in the presence of a hypoenhancing mass (Fig 14). Ductal carcinoma should be suspected when there is invasion and dilatation of the main pancreatic duct and the abrupt cutoff sign associated with pancreatic atrophy. PDP shows smooth progressive narrowing of the main

pancreatic duct and the distal bile duct. Vascular encasement favors diagnosis of PDAC.

Autoimmune Pancreatitis

AIP is a distinct type of chronic pancreatitis characterized by lymphoplasmacytic infiltration and fibrosis at histologic evaluation and excellent response to treatment with corticosteroids (48). The incidence and prevalence of AIP is unclear, although it has been underdiagnosed. AIP was identified in approximately 6%–8% of pancreatic resections for suspected pancreatic cancer in Japan (49). In the United States, a reported frequency of 11% of pancreatic resections for benign indications showed AIP at histopathologic analysis (50).

AIP is classified into two subtypes. Type 1 AIP demonstrates lymphoplasmacytic sclerosing pancreatitis, with infiltration of lymphocytes and plasmacytes (especially immunoglobulin G4 [IgG4]) and is the pancreatic manifestation of IgG4-related disease. Type 2 AIP affects younger patients (mean age, 43 years) (51,52). Type 1 AIP is often associated with extrapancreatic manifestations, with involvement of the biliary tree (68%–88%), kidneys (35%) (Fig 16), retroperitoneum (10%–20%), and salivary or lacrimal glands (12%–16%) and helps to differentiate it from PDAC (53–56). Type 2 AIP may be associated with inflammatory bowel disease, particularly ulcerative colitis, and patients with type 2 AIP may have a normal IgG4 level. Type 2 AIP may mimic PDAC, but it is seen in younger patients (56).

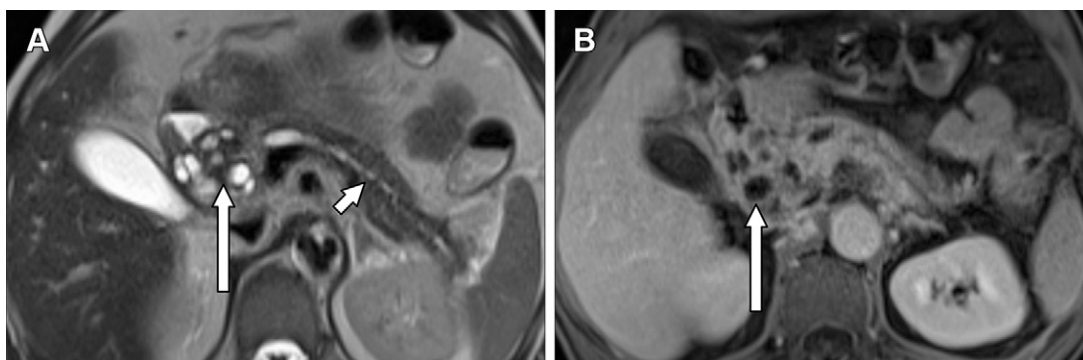


Figure 13. Cystic pattern of PDP in a 50-year-old man with right upper quadrant pain and weight loss for 9 months. (A) Axial T2-weighted image shows prominent tissue in the groove, with cystic changes (long arrow). The pancreatic duct is dilated (short arrow). (B) Axial contrast-enhanced T1-weighted fat-suppressed MR image shows the cysts and heterogeneous enhancement in the groove (arrow).

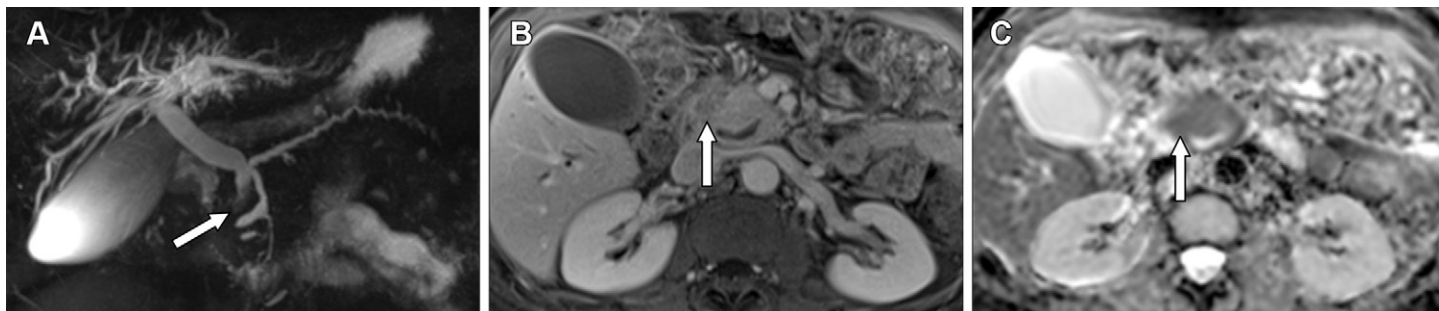


Figure 14. Paraduodenal pancreatic cancer in a 62-year-old man presenting with jaundice and findings of hyperbilirubinemia, with common bile duct dilatation demonstrated at US of the right upper quadrant of the abdomen (not shown). (A) Coronal MRCP image shows the double duct sign from a dilated common bile duct and pancreatic duct extending to the level of the ampulla (arrow). (B) Axial contrast-enhanced T1-weighted MR image shows a hypoenhancing lesion involving the paraduodenal groove between the pancreatic head and the duodenum (arrow). (C) Axial apparent diffusion coefficient map shows low signal intensity (arrow) from restricted diffusion. The absence of cysts and the double duct sign in this patient presenting without a history of alcohol over-consumption raised concern for cancer, and subsequent biopsy showed PDAC.

Table 2: Differentiating PDP from PDAC

Feature	PDP	PDAC
Involvement of pancreaticoduodenal groove	Involved	Less frequently involved
Delayed progressive enhancing fibrotic tissue	Often patchy and heterogeneous	Homogeneously hypoattenuating or hypointense
Association with cysts	Associated with cysts	Cysts are rare
Vascular involvement	Not usually associated	Associated
Relationship to common bile duct	Displaces but rarely obstructs	Invades and obstructs

Sources.—References 36, 44, and 45.

Therapy for AIP typically involves treatment with high-dose steroids, with a response observed at imaging as early as 2 weeks after steroid treatment begins. Nonresolution of imaging abnormalities or clinical symptoms should raise concern for alternative diagnoses, such as PDAC (52).

At imaging, AIP may show three distinct patterns of pancreatic involvement: diffuse (70% of the pancreas), focal (up to 30% in type 1 and 80% in type 2), and multifocal (5%) (52). Diffuse enlargement of the pancreas, with an enlarged tail, loss of normal lobulations, and a “sausage-shaped” appearance, and a capsule-like rim are the most classic imaging features of AIP, but they are only seen in 30%–40% of cases (52,57).

AIP may be difficult to distinguish from PDAC at imaging, because both can appear as focal (Figs 16, 17, S4) or infiltrative mass (Fig 18) (Table 3) (51,56–58). Features favoring AIP include homogeneous enhancement during the portal venous phase, a hypointense capsule-like rim, extrapancreatic man-

ifestations (Fig 16), the absence of pancreatic atrophy, and excellent response to steroid treatment (48,52,56–58). Ductal findings favoring focal AIP include the “duct-penetrating” sign (best seen using secretin-enhanced MRCP); only mild dilatation of the main pancreatic duct, usually limited to an area of less than 4 mm; longer length of the narrowing of the main pancreatic duct (3 cm or more) in the involved segment of the pancreas, without an abrupt cutoff; the enhanced duct sign (wall enhancement of the main pancreatic duct in the lesion); multiple areas of narrowing or strictures of the main pancreatic duct; and the “icicle sign” (smoothly tapered narrowing of the upstream pancreatic duct) (59). When AIP is associated with biliary involvement, the imaging appearance can mimic primary sclerosing cholangitis. Multiple pancreatic lesions also favor a diagnosis of AIP over that of PDAC. Vascular encasement, fluid collections, or an increased number of lymph nodes are rare with AIP and favor a diagnosis of PDAC.

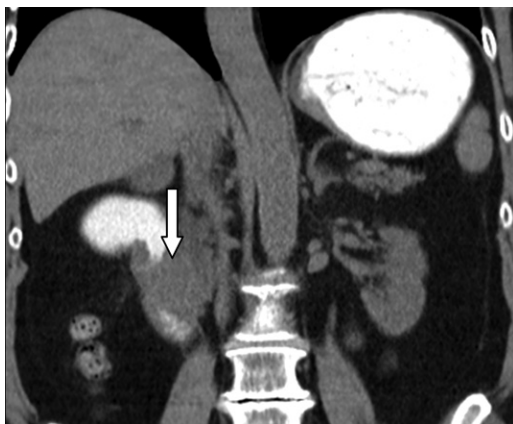


Figure 15. PDP mimicking PDAC in a 56-year-old man. Coronal unenhanced CT image with oral contrast material shows a lesion in the pancreatic groove and obstruction at the second portion of the duodenum (arrow). The lack of cysts makes the diagnosis more difficult, and biopsy was performed.

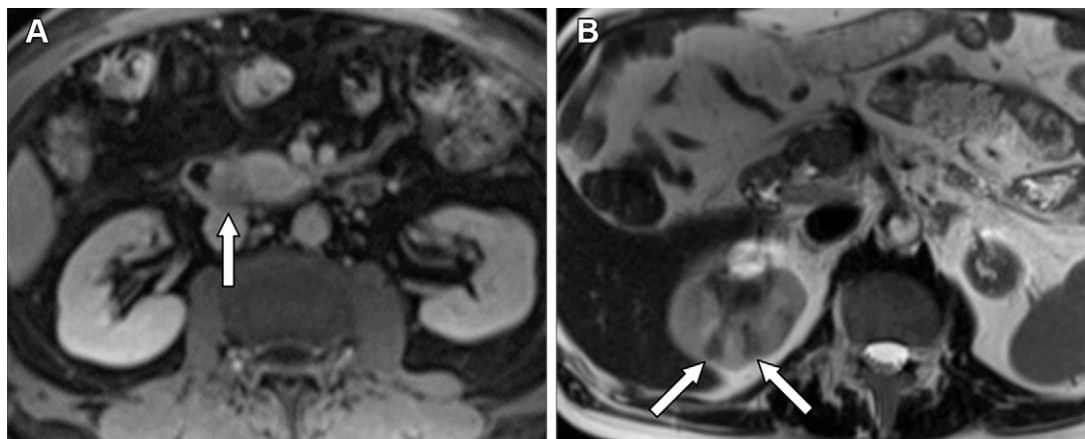


Figure 16. AIP in a 72-year-old man. (A) Axial contrast-enhanced T1-weighted fat-suppressed MR image shows a hypointense peripancreatic mass (arrow) in the pancreaticoduodenal groove. (B) Axial T2-weighted MR image shows associated renal-cortical hypointense areas (arrows) suggestive of tubulointerstitial nephritis from renal involvement of immunoglobulin G4 (IgG4)-related disease. The renal findings help to distinguish this entity from PDAC or PDP.

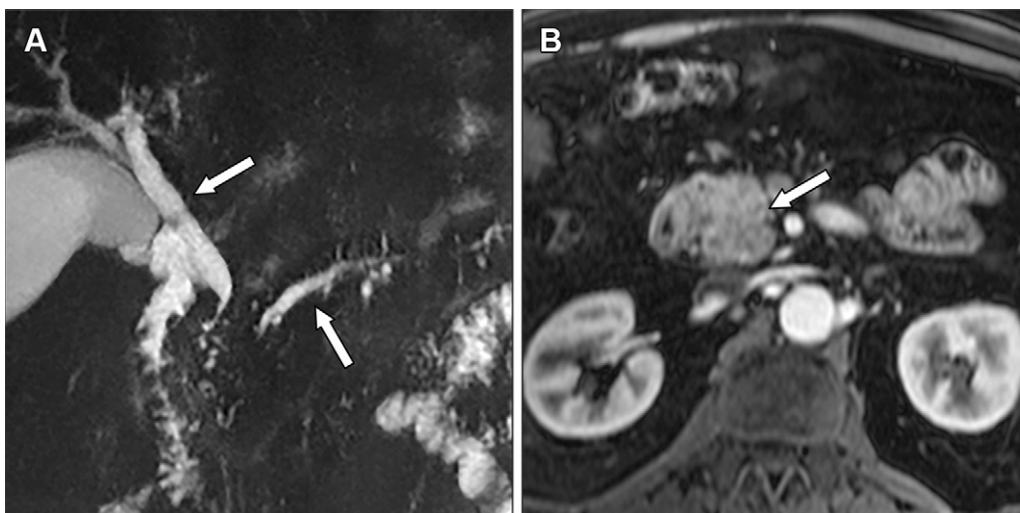


Figure 17. AIP in a 62-year-old man with a history of obstructive jaundice and an elevated CA 19-9 level. (A) MRCP image shows the double duct sign suggestive of PDAC with a dilated common duct (upper arrow) and the pancreatic duct (lower arrow). (B) Axial early contrast-enhanced T1-weighted fat-suppressed MR image shows a subtle mild hypointense mass (arrow). The patient was suspected to have PDAC but at the Whipple procedure was found to have AIP.

At DWI, AIP appears as diffuse, solitary, or multifocal hyperintensities, while PDAC usually is a solitary focal lesion (56). Choi et al (60) reported that the duct-penetrating sign, homogeneous enhancement in the portal phase, and a low apparent diffusion coefficient (cutoff value, $0.94 \times 10^{-3} \text{ mm}^2/\text{sec}$) as significant independent variables to differentiate focal AIP from PDAC, and that using two or three of these criteria resulted in specificity of more than 98%. Newer techniques involving radiomics analysis are being developed to differentiate focal AIP from PDAC, but further validation is needed (61,62). Fluorine

18 fluorodeoxyglucose (FDG) PET shows uptake in AIP and the extrapancreatic lesions, unlike PDAC, which shows uptake in the tumor and metastases. Improvement of the appearance of AIP lesions on PET images can be seen after steroid treatment. Although imaging and clinical features can be suggestive of AIP, biopsy may be required for definitive diagnosis.

Pancreatic Neuroendocrine Tumor

Pancreatic neuroendocrine tumors (PanNETs) are rare neoplasms but are the second most common solid pancreatic

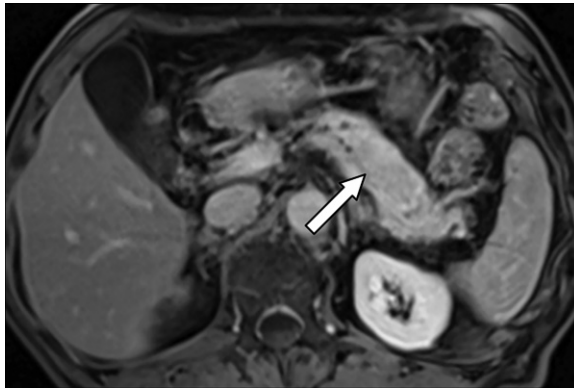


Figure 18. AIP mimicking infiltrative PDAC in a 79-year-old man. Axial contrast-enhanced T1-weighted fat-suppressed MR image shows a heterogeneous 4.4-cm ill-defined masslike lesion (arrow) mimicking PDAC. Biopsy results showed AIP.

Table 3: Differentiating AIP from PDAC

Feature	AIP	PDAC
Pancreatic involvement	Diffuse, focal, or multifocal	Focal, infrequently multifocal or diffuse
Shape	Typically sausage shaped	Not sausage shaped
Capsule-like rim	Present	Absent
Dilated pancreatic duct	Generally not present (<4 mm)	Present (>4 mm)
Pancreatic duct appearance	Duct-penetrating sign may be present	Abruptly terminating pancreatic duct
Main pancreatic duct features	Multifocal narrowing or strictures with skip areas and longer length of narrowing (>3 cm)	Stricture with abrupt cutoff
Vascular involvement	Lacks vascular involvement	Associated with vascular involvement
Pancreatic atrophy	Lacks pancreatic atrophy (unless treated)	Upstream pancreatic atrophy
Biliary involvement	Mimics primary sclerosing cholangitis, enhancing bile duct wall	Dilatation may result from pancreatic mass or metastasis without enhancing wall
Extrapancreatic involvement	May suggest diagnosis: biliary strictures, renal lesions, retroperitoneal soft-tissue mimicking retroperitoneal fibrosis; involvement of prostate, lungs, and salivary or lacrimal glands	Metastases: liver or lung lesions, lymphadenopathy, peripancreatic or peritoneal metastases
Lymphadenopathy	Absent	Present
Immunoglobulin G4 (IgG4) level	Associated with elevated level	Usually normal
Ca 19-9 level	Not elevated	Elevated
Response to steroids	Yes	No

Sources.—References 51, 56–58.

tumor after PDAC (Table 4) (63–66). PanNETs are divided into two broad but distinct categories on the basis of their morphology: (a) less aggressive types such as well-differentiated PanNETs (previously known as “islet cell tumors,” usually with low proliferative activity [median Ki-67, <5%]) and PanNET grade 3 tumors with higher proliferative activity (Ki > 20%), which occur rarely and (b) more aggressive high-grade poorly differentiated carcinomas with an extremely high proliferative index (usually Ki-67 > 50%). PanNETs are also clinically divided into functional and nonfunctional neoplasms on the basis of hormone production and associated clinical syndromes. Insulinomas and gastrinomas are the most common functioning tumors. Nonfunctioning tumors are more common and account for two-thirds of all PanNETs (63).

The imaging features of PanNETs are variable. When they are homogeneously enhancing during the arterial phase at CT and MRI, PanNETs are readily distinguished from PDACs, which tend to be hypovascular. However, PanNETs may not

show the classic hypervascular or T2-hyperintense appearance (Fig 19) and may mimic PDACs when they are hypovascular or rim enhancing (Fig 20) (65). The high T2 signal intensity seen in cystic PanNETs is not typically seen in PDACs (Fig 21).

PanNETs can be atypical and hypovascular in 41.5% of cases and can be difficult to distinguish from PDACs (64). Unlike PDACs, PanNETs do not originate from the pancreatic ductal epithelium and do not cause pancreatic duct dilatation until they are large enough to exert mass effect on the duct. In addition, PanNETs are usually encapsulated and not associated with pancreatic atrophy as PDACs are. However, small neuroendocrine tumors can cause ductal dilatation and obstruction and upstream pancreatic atrophy secondary to secretion of serotonin and other metabolites, causing fibrotic narrowing of the main pancreatic duct. Marked pancreatic duct dilatation and stenosis and pancreatic atrophy out of proportion to an underlying hypervascular mass suggest a serotonin-producing PanNET. However, the underlying mass may not be identified at CT and requires MRI or

Table 4: Differentiating Neuroendocrine Tumors from PDACs

Feature	Neuroendocrine Tumor	PDAC
Vascularity	Classically hypervascular	Hypovascular
Hyperintensity	Classically T2 hyperintense	Generally not T2 hyperintense
No. of masses	May be multiple	Usually solitary mass
Mass definition	Usually well defined	Mass may be less well defined and infiltrative
Cysts and calcifications	Can be cystic and have a thick enhancing wall or calcifications	Rarely cystic or with calcifications
Hemorrhage	May be present	Rarely present
Pancreatic duct obstruction	Typically none	Associated with obstruction
Biliary obstruction	Usually absent	May be present when it involves the head of the pancreas
Vascular encasement	Rarely present	Associated with vascular encasement
Pancreatic atrophy	In rare cases	Associated with pancreatic atrophy
Appearance of liver metastases	Hypervascular	Hypovascular
Association with hormone production	May be associated	Not associated

Sources.—References 63–66.



Figure 19. PanNET in a 25-year-old man with a history of jaundice. (A) Axial contrast-enhanced T1-weighted fat-suppressed MR image shows a hypoenhancing pancreatic head lesion (arrow) mimicking PDAC. (B) Coronal three-dimensional navigator-triggered MRCP image shows the double duct sign (arrow). (C) Coronal T2-weighted MR image shows a hypointense lesion (arrow). Because the patient is younger than those with PDAC, the diagnosis is more likely to be a PanNET. This well-differentiated grade 2 PanNET does not show the classic hypervascularity or T2-hyperintense appearance associated with these lesions, and instead mimics a PDAC.

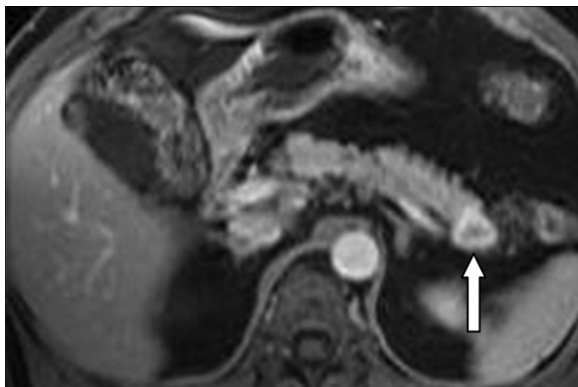


Figure 20. PanNET in a 62-year-old woman with a history of a cystic lesion of the pancreatic tail seen at CT. Axial T1-weighted fat-suppressed contrast-enhanced MR image shows a rim-enhancing lesion in the pancreatic tail (arrow) that proved to be a PanNET at fine-needle aspiration biopsy.

endoscopic US for visualization (Fig 22) (67). Jeon et al (66) reported higher frequencies in nonhypervascular PanNETs of portal hyper- or iso-enhancement in comparison with that

of the parenchyma, well-defined margins, and maximal upstream parenchymal thickness of 10 mm or greater when compared with PDACs. Vascular invasion tends to favor a diagnosis of PDAC.

Solid Pseudopapillary Neoplasm

Solid pseudopapillary neoplasms, also referred to as solid and papillary epithelial neoplasms of the pancreas, are rare, accounting for 1%–2% of all pancreatic tumors (68). Unlike PDACs, solid pseudopapillary neoplasms tend to manifest in young women (mean age, 28.5 years at presentation) (69) and show a low potential for malignant transformation. The behavior and prognosis of solid pseudopapillary neoplasms are generally favorable.

Solid pseudopapillary neoplasms tend to be large at presentation (2.5–17.0 cm; mean size, 9 cm) and well defined (11), and they can be found throughout the pancreas. Large lesions can be distinguished from PDACs because they contain solid and cystic components due to hemorrhage, necrosis, and cystic degeneration (70,71). Small solid pseudopapillary neoplasms (size, <3 cm) usually have sharp margins

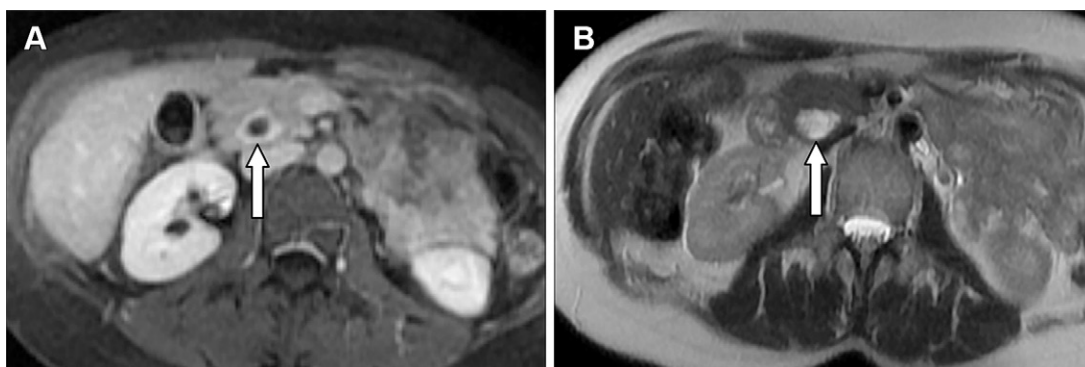


Figure 21. Cystic PanNET in a 46-year-old woman. (A) Axial early contrast-enhanced T1-weighted fat-suppressed MR image shows a rim-enhancing lesion mimicking PDAC (arrow). (B) Axial T2-weighted MR image shows a high-signal-intensity cystic component (arrow) more typical of a cystic PanNET than PDAC.

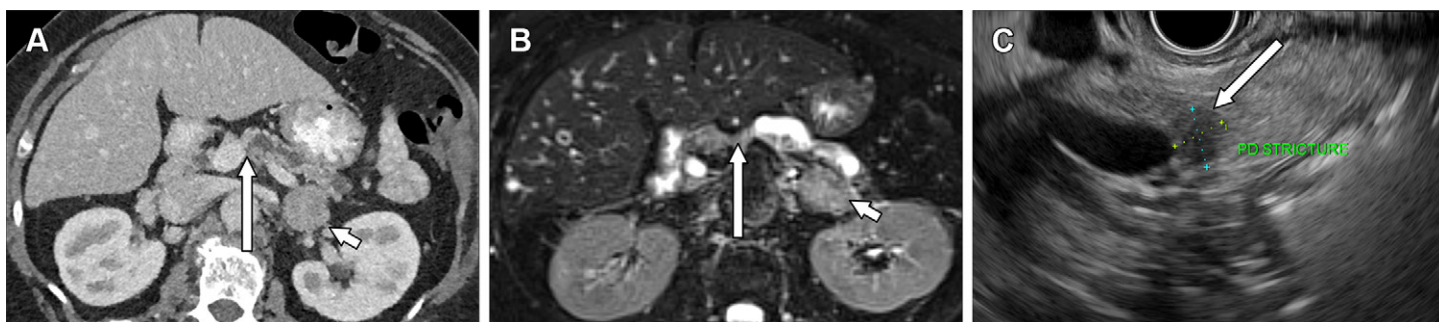


Figure 22. Serotonin-producing carcinoid PanNET in a 66-year-old woman with a history of an incidental adrenal adenoma. (A) Axial contrast-enhanced CT image shows pancreatic duct dilatation with associated marked atrophy, without a discrete mass (long arrow). An incidental 2.9-cm left adrenal lesion (short arrow) is also present and represented an adenoma on in- and opposed-phase CT images (not shown). (B) Axial T2-weighted fat-suppressed MR image shows a dilated pancreatic duct with abrupt termination (long arrow) and marked pancreatic atrophy. It is difficult to identify an underlying mass, but given the markedly dilated duct and abrupt termination, the findings are concerning for underlying cancer. (C) Endoscopic US was performed and a small hypoechoic mass was identified with pathology demonstrating a serotonin-producing NET (long arrow). Biopsy showed World Health Organization (WHO) grade 1 (carcinoid) PanNET, which is a rare entity.

and gradual enhancement in the portal venous phase (70,71). When solid and papillary epithelial neoplasms lack hemorrhagic components or necrosis, they may appear nonspecific and mimic PDACs or other lesions such as PanNETs (Fig 23).

Compared with PDACs, solid pseudopapillary neoplasms often occur in younger patients. They are typically large at diagnosis, often associated with hemorrhage, and well defined and encapsulated, without metastases. Unlike PDACs, solid pseudopapillary neoplasms are less commonly associated with pancreatic and biliary duct dilatation, upstream parenchymal atrophy, or vascular invasion (72). Biopsy may be required for definitive diagnosis.

Metastases Involving the Pancreas

Metastases to the pancreas are rare, accounting for 2%–5% of pancreatic malignancies, and most commonly occur from renal cell carcinoma (73). Pancreatic metastatic disease may be a single tumor (Fig 24) or multiple tumors, or it may involve the pancreas diffusely and have a variable appearance, depending on the primary site. Metastases from hypovascular or hypoenhancing primary malignancies (lung, breast, and colorectal cancer) can mimic PDAC, while hypervascular or arterially enhancing neoplasms (eg, renal cell carcinoma; melanoma; breast, thyroid, or hepatocellular carcinoma; and osteosarcoma) are typically hyperenhancing and multiple tumors, unlike PDACs (74). At US, metastases appear as solid hypoechoic lesions. Contrast-enhanced US allows better visualization of metastases

from hypervascular tumors. At contrast-enhanced CT and MRI, hypervascular pancreatic metastasis demonstrates homogeneous enhancement when the tumors are small, and rim enhancement when they are larger (75). Metastases from the clear cell variant of renal cell carcinoma may show microscopic fat at chemical shift MRI (Fig S5) and may appear more than 10 years after the patient underwent nephrectomy, while PDACs and PanNETs do not typically contain fat (76). Metastases that invade the ductal epithelium and obstruct the pancreatic duct can mimic PDAC.

Unlike PDAC, metastases are usually well circumscribed, with little to no pancreatic duct obstruction; lack vascular invasion; and often have multiple sites of involvement in the pancreas and other organs. Biopsy may be required for confirmation, especially when suspected hypovascular metastasis mimics PDAC.

Lymphoma

Pancreatic lymphoma can be primary or secondary. Primary pancreatic lymphoma is rare and usually non-Hodgkin lymphoma. Secondary pancreatic lymphoma is more common and occurs when there is pancreatic involvement by lymphoma from adjacent lymph nodes or organs. Lymphoma can manifest as a focal mass, multiple masses, or diffuse infiltration.

Diffuse infiltrating pancreatic lymphoma may mimic pancreatitis, while focal masslike lymphoma can mimic PDAC. Masslike lymphoma often occurs in the pancreatic head and,



Figure 23. Solid pseudopapillary neoplasm in a 19-year-old woman. Axial parenchymal phase contrast-enhanced CT image shows a hypoattenuating 2.5-cm mass (arrow) mimicking PDAC. The age of the patient and the well-circumscribed lesion is more typical of a solid pseudopapillary neoplasm than PDAC.



Figure 25. Lymphoma in a 64-year-old woman. Axial contrast-enhanced CT image shows diffuse enlargement of the pancreas with well-defined hypoenhancing masses (arrows) from large B-cell lymphoma based on biopsy results.

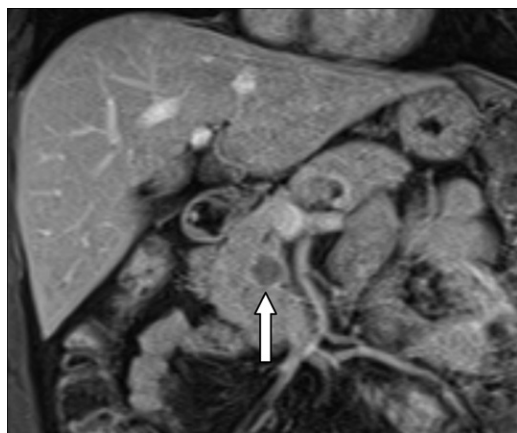


Figure 24. Metastatic disease to the pancreas in a 54-year-old man with a history of melanoma of the lower extremity. Coronal contrast-enhanced T1-weighted fat-suppressed MR image shows a 2.3-cm hypoenhancing lesion (arrow) that was new compared with the prior study and mimics PDAC but was biopsied and was proven to represent melanoma metastasis.

similar to PDAC, hypoenhances at CT and MRI compared with the background pancreas. Lymphomatous lesions tend to show mild to moderate homogeneous enhancement, are T1 hypointense and mildly T2 hyperintense, and restrict diffusion. Calcifications are uncommon in untreated lymphoma (77).

Lymphoma should be suspected over PDAC when there is a bulky localized well-defined tumor with no significant pancreatic duct dilatation, unlike PDAC, which tends to be ill defined, with an irregular contour (Fig 25). Pancreatic lymphoma may surround the bowel and vessels without leading to obstruction or occlusion, which differs from PDAC, in which bowel obstruction and vascular encasement is common (77). Furthermore, lymphoma more frequently has retroperitoneal lymph node involvement and lymphadenopathy below the renal vein level and lacks cystic changes, necrosis, and invasive tumor growth. Organ involvement such as renal or perirenal disease is often associated with lymphoma but not with PDAC. Definitive diagnosis requires biopsy.

Conclusion

Radiologists should recognize the typical and atypical imaging features of PDAC and its mimics to distinguish among these entities. Imaging features may favor diagnosis of one entity, and biopsy may be required to reach a final diagnosis to ensure proper management and treatment.

Author affiliations.—From the Department of Radiology, Northwestern Memorial Hospital, Northwestern University Feinberg School of Medicine, 676 N St. Clair St, Ste 800, Chicago, IL 60611 (F.H.M., C.L.V., N.A.H., P.N., A.J.); and Department of Radiology and Imaging, Medical College of Georgia, Augusta, GA (P.K.M.). Presented as an education exhibit at the 2022 RSNA Annual Meeting. Received March 16, 2023; revision requested May 2 and received June 1; accepted June 16. **Address correspondence to** F.H.M. (email: Frank.Miller@nm.org).

Disclosures of conflicts of interest.—The authors, editor, and reviewers have disclosed no relevant relationships.

References

1. Afghani E, Klein AP. Pancreatic adenocarcinoma: trends in epidemiology, risk factors, and outcomes. *Hematol Oncol Clin North Am* 2022;36(5):879–895.
2. Johnston A, Serhal A, Lopes Vendrami C, et al. The abrupt pancreatic duct cutoff sign on MDCT and MRI. *Abdom Radiol (NY)* 2020;45(8):2476–2484.
3. Kleeff J, Korc M, Apte M, et al. Pancreatic cancer. *Nat Rev Dis Primers* 2016;2(1):16022.
4. Ishigami K, Yoshimitsu K, Irie H, et al. Diagnostic value of the delayed phase image for iso-attenuating pancreatic carcinomas in the pancreatic parenchymal phase on multidetector computed tomography. *Eur J Radiol* 2009;69(1):139–146.
5. Almeida RR, Lo GC, Patino M, Bizzo B, Canellas R, Sahani DV. Advances in pancreatic CT imaging. *AJR Am J Roentgenol* 2018;211(1):52–66.
6. Al-Hawary MM, Kaza RK, Azar SF, Ruma JA, Francis IR. Mimics of pancreatic ductal adenocarcinoma. *Cancer Imaging* 2013;13(3):342–349.
7. Brook OR, Gourtsoyianni S, Brook A, Siewert B, Kent T, Raptopoulos V. Split-bolus spectral multidetector CT of the pancreas: assessment of radiation dose and tumor conspicuity. *Radiology* 2013;269(1):139–148.
8. Nishiharu T, Yamashita Y, Abe Y, et al. Local extension of pancreatic carcinoma: assessment with thin-section helical CT versus with breath-hold fast MR imaging—ROC analysis. *Radiology* 1999;212(2):445–452.
9. Park MJ, Kim YK, Choi SY, Rhim H, Lee WJ, Choi D. Preoperative detection of small pancreatic carcinoma: value of adding diffusion-weighted imaging to conventional MR imaging for improving confidence level. *Radiology* 2014;273(2):433–443.
10. Takakura K, Sumiyama K, Munakata K, et al. Clinical usefulness of diffusion-weighted MR imaging for detection of pancreatic cancer: comparison with enhanced multidetector-row CT. *Abdom Imaging* 2011;36(4):457–462.
11. O'Neill E, Hammond N, Miller FH. MR imaging of the pancreas. *Radiol Clin North Am* 2014;52(4):757–777.

12. Sandrasegaran K, Lin C, Akisik FM, Tann M. State-of-the-art pancreatic MRI. *AJR Am J Roentgenol* 2010;195(1):42–53.
13. Kobi M, Veillette G, Narurkar R, et al. Imaging and management of pancreatic cancer. *Semin Ultrasound CT MR* 2020;41(2):139–151.
14. Gangi S, Fletcher JG, Nathan MA, et al. Time interval between abnormalities seen on CT and the clinical diagnosis of pancreatic cancer: retrospective review of CT scans obtained before diagnosis. *AJR Am J Roentgenol* 2004;182(4):897–903.
15. Toshima F, Watanabe R, Inoue D, et al. CT abnormalities of the pancreas associated with the subsequent diagnosis of clinical stage I pancreatic ductal adenocarcinoma more than 1 year later: a case-control study. *AJR Am J Roentgenol* 2021;217(6):1353–1364.
16. Wang Y, Miller FH, Chen ZE, et al. Diffusion-weighted MR imaging of solid and cystic lesions of the pancreas. *RadioGraphics* 2011;31(3):E47–E64 [Published correction appears in *Radiographics* 2011;31(5):1496.]
17. Siddiqui N, Vendrami CL, Chatterjee A, Miller FH. Advanced MR imaging techniques for pancreas imaging. *Magn Reson Imaging Clin N Am* 2018;26(3):323–344.
18. Wang Y, Chen ZE, Nikolaidis P, et al. Diffusion-weighted magnetic resonance imaging of pancreatic adenocarcinomas: association with histopathology and tumor grade. *J Magn Reson Imaging* 2011;33(1):136–142.
19. Marion-Audibert AM, Vullierme MP, Ronot M, et al. Routine MRI with DWI sequences to detect liver metastases in patients with potentially resectable pancreatic ductal carcinoma and normal liver CT: a prospective multicenter study. *AJR Am J Roentgenol* 2018;211(5):W217–W225.
20. Kim JH, Park SH, Yu ES, et al. Visually isoattenuating pancreatic adenocarcinoma at dynamic-enhanced CT: frequency, clinical and pathologic characteristics, and diagnosis at imaging examinations. *Radiology* 2010;257(1):87–96.
21. Yoon SH, Lee JM, Cho JY, et al. Small (≤ 20 mm) pancreatic adenocarcinomas: analysis of enhancement patterns and secondary signs with multiphasic multidetector CT. *Radiology* 2011;259(2):442–452.
22. Hata H, Mori H, Matsumoto S, et al. Fibrous stroma and vascularity of pancreatic carcinoma: correlation with enhancement patterns on CT. *Abdom Imaging* 2010;35(2):172–180.
23. Gong XH, Xu JR, Qian LJ. Atypical and uncommon CT and MR imaging presentations of pancreatic ductal adenocarcinoma. *Abdom Radiol (NY)* 2021;46(9):4226–4237.
24. Prokesch RW, Chow LC, Beaulieu CF, Bammer R, Jeffrey RB Jr. Isoattenuating pancreatic adenocarcinoma at multi-detector row CT: secondary signs. *Radiology* 2002;224(3):764–768.
25. Tamada T, Ito K, Kanomata N, et al. Pancreatic adenocarcinomas without secondary signs on multiphasic multidetector CT: association with clinical and histopathologic features. *Eur Radiol* 2016;26(3):646–655.
26. Haj-Mirzaian A, Kawamoto S, Zaheer A, Hruban RH, Fishman EK, Chu LC. Pitfalls in the MDCT of pancreatic cancer: strategies for minimizing errors. *Abdom Radiol (NY)* 2020;45(2):457–478.
27. Kosmahl M, Pauser U, Anlauf M, Klöppel G. Pancreatic ductal adenocarcinomas with cystic features: neither rare nor uniform. *Mod Pathol* 2005;18(9):1157–1164.
28. Miller FH, Lopes Vendrami C, Recht HS, et al. Pancreatic cystic lesions and malignancy: assessment, guidelines, and the field defect. *RadioGraphics* 2022;42(1):87–105.
29. Javadi S, Menias CO, Korivi BR, et al. Pancreatic calcifications and calcified pancreatic masses: pattern recognition approach on CT. *AJR Am J Roentgenol* 2017;209(1):77–87.
30. Miyoshi H, Kano M, Kobayashi S, et al. Diffuse pancreatic cancer mimicking autoimmune pancreatitis. *Intern Med* 2019;58(17):2523–2527.
31. Siddiqui AJ, Miller F. Chronic pancreatitis: ultrasound, computed tomography, and magnetic resonance imaging features. *Semin Ultrasound CT MR* 2007;28(5):384–394.
32. Wolske KM, Ponnatapura J, Kolokythas O, Burke LMB, Tappouni R, Lalwani N. Chronic pancreatitis or pancreatic tumor? a problem-solving approach. *RadioGraphics* 2019;39(7):1965–1982.
33. Elmas N, Oran I, Oyar O, Ozer H. A new criterion in differentiation of pancreatitis and pancreatic carcinoma: artery-to-vein ratio using the superior mesenteric vessels. *Abdom Imaging* 1996;21(4):331–333.
34. Ichikawa T, Sou H, Araki T, et al. Duct-penetrating sign at MRCP: usefulness for differentiating inflammatory pancreatic mass from pancreatic carcinomas. *Radiology* 2001;221(1):107–116.
35. Schima W, Böhm G, Rösch CS, Klaus A, Függer R, Kopf H. Mass-forming pancreatitis versus pancreatic ductal adenocarcinoma: CT and MR imaging for differentiation. *Cancer Imaging* 2020;20(1):52.
36. Perez-Johnston R, Sainani NI, Sahani DV. Imaging of chronic pancreatitis (including groove and autoimmune pancreatitis). *Radiol Clin North Am* 2012;50(3):447–466.
37. Miller FH, Keppke AL, Wadhwa A, Ly JN, Dalal K, Kamler VA. MRI of pancreatitis and its complications: part 2, chronic pancreatitis. *AJR Am J Roentgenol* 2004;183(6):1645–1652.
38. Kirkegård J, Mortensen FV, Cronin-Fenton D. Chronic pancreatitis and pancreatic cancer risk: a systematic review and meta-analysis. *Am J Gastroenterol* 2017;112(9):1366–1372.
39. Vanek P, Urban O, Trikudanathan G, Freeman ML. Disconnected pancreatic duct syndrome in patients with necrotizing pancreatitis. *Surg Open Sci* 2022;11:19–25.
40. Munigala S, Kanwal F, Xian H, Scherrer JF, Agarwal B. Increased risk of pancreatic adenocarcinoma after acute pancreatitis. *Clin Gastroenterol Hepatol* 2014;12(7):1143–1150.e1.
41. Kimura Y, Kikuyama M, Kodama Y. Acute pancreatitis as a possible indicator of pancreatic cancer: the importance of mass detection. *Intern Med* 2015;54(17):2109–2114.
42. Li S, Tian B. Acute pancreatitis in patients with pancreatic cancer: Timing of surgery and survival duration. *Medicine (Baltimore)* 2017;96(3):e5908.
43. Levenick JM, Gordon SR, Sutton JE, Suriawinata A, Gardner TB. A comprehensive, case-based review of groove pancreatitis. *Pancreas* 2009;38(6):e169–e175.
44. Mittal PK, Harri P, Nandwana S, et al. Paraduodenal pancreatitis: benign and malignant mimics at MRI. *Abdom Radiol (NY)* 2017;42(11):2652–2674.
45. Kalb B, Martin DR, Sarmiento JM, et al. Paraduodenal pancreatitis: clinical performance of MR imaging in distinguishing from carcinoma. *Radiology* 2013;269(2):475–481.
46. Adsay NV, Zamboni G. Paraduodenal pancreatitis: a clinico-pathologically distinct entity unifying “cystic dystrophy of heterotopic pancreas”, “para-duodenal wall cyst”, and “groove pancreatitis”. *Semin Diagn Pathol* 2004;21(4):247–254.
47. Muraki T, Kim GE, Reid MD, et al. Paraduodenal pancreatitis: imaging and pathologic correlation of 47 cases elucidates distinct subtypes and the factors involved in its etiopathogenesis. *Am J Surg Pathol* 2017;41(10):1347–1363.
48. Okazaki K, Kawa S, Kamisawa T, et al; Members of the research committee for IgG4-related disease supported by the Ministry of Health, Labour, Welfare of Japan, Japan Pancreas Society. Amendment of the Japanese consensus guidelines for autoimmune pancreatitis, 2020. *J Gastroenterol* 2022;57(4):225–245.
49. Nishimori I, Tamakoshi A, Otsuki M; Research Committee on Intractable Diseases of the Pancreas, Ministry of Health, Labour, and Welfare of Japan. Prevalence of autoimmune pancreatitis in Japan from a nationwide survey in 2002. *J Gastroenterol* 2007;42(Suppl 18):6–8.
50. Yadav D, Notahara K, Smyrk TC, et al. Idiopathic tumefactive chronic pancreatitis: clinical profile, histology, and natural history after resection. *Clin Gastroenterol Hepatol* 2003;1(2):129–135.
51. Sandrasegaran K, Menias CO. Imaging in autoimmune pancreatitis and immunoglobulin G4-related disease of the abdomen. *Gastroenterol Clin North Am* 2018;47(3):603–619.
52. Khandelwal A, Inoue D, Takahashi N. Autoimmune pancreatitis: an update. *Abdom Radiol (NY)* 2020;45(5):1359–1370.
53. Hafezi-Nejad N, Singh VK, Fung C, Takahashi N, Zaheer A. MR imaging of autoimmune pancreatitis. *Magn Reson Imaging Clin N Am* 2018;26(3):463–478.
54. Agrawal S, Daruwala C, Khurana J. Distinguishing autoimmune pancreatitis from pancreaticobiliary cancers: current strategy. *Ann Surg* 2012;255(2):248–258.
55. Manfredi R, Frulloni L, Mantovani W, Bonatti M, Graziani R, Pozzi Mucelli R. Autoimmune pancreatitis: pancreatic and extrapancreatic MR imaging-MR cholangiopancreatography findings at diagnosis, after steroid therapy, and at recurrence. *Radiology* 2011;260(2):428–436.
56. Lopes Vendrami C, Shin JS, Hammond NA, Kothari K, Mittal PK, Miller FH. Differentiation of focal autoimmune pancreatitis from pancreatic ductal adenocarcinoma. *Abdom Radiol (NY)* 2020;45(5):1371–1386.
57. Takahashi N, Fletcher JG, Hough DM, et al. Autoimmune pancreatitis: differentiation from pancreatic carcinoma and normal pancreas on the basis of enhancement characteristics at dual-phase CT. *AJR Am J Roentgenol* 2009;193(2):479–484.
58. Kothari K, Lopes Vendrami C, Kelahan LC, Shin JS, Mittal P, Miller FH. Inflammatory mimickers of pancreatic adenocarcinoma. *Abdom Radiol (NY)* 2020;45(5):1387–1396.
59. Kim HJ, Kim YK, Jeong WK, Lee WJ, Choi D. Pancreatic duct “Icicle sign” on MRI for distinguishing autoimmune pancreatitis from pancreatic ductal adenocarcinoma in the proximal pancreas. *Eur Radiol* 2015;25(6):1551–1560.
60. Choi SY, Kim SH, Kang TW, Song KD, Park HJ, Choi YH. Differentiating mass-forming autoimmune pancreatitis from pancreatic ductal adenocarcinoma on the basis of contrast-enhanced MRI and DWI findings. *AJR Am J Roentgenol* 2016;206(2):291–300.
61. Li J, Liu F, Fang X, et al. CT radiomics features in differentiation of focal-type autoimmune pancreatitis from pancreatic ductal adenocarcinoma: a propensity score analysis. *Acad Radiol* 2022;29(3):358–366.
62. Shiraishi M, Igarashi T, Hiroaki F, Oe R, Ohki K, Ojiri H. Radiomics based on diffusion-weighted imaging for differentiation between

- focal-type autoimmune pancreatitis and pancreatic carcinoma. *Br J Radiol* 2022;95(1140):20210456.
63. Ciaravino V, De Robertis R, Tinazzi Martini P, et al. Imaging presentation of pancreatic neuroendocrine neoplasms. *Insights Imaging* 2018;9(6):943–953.
 64. Li J, Lu J, Liang P, et al. Differentiation of atypical pancreatic neuroendocrine tumors from pancreatic ductal adenocarcinomas: Using whole-tumor CT texture analysis as quantitative biomarkers. *Cancer Med* 2018;7(10):4924–4931.
 65. Herwick S, Miller FH, Keppke AL. MRI of islet cell tumors of the pancreas. *AJR Am J Roentgenol* 2006;187(5):W472–W480.
 66. Jeon SK, Lee JM, Joo I, et al. Nonhypervascular Pancreatic Neuroendocrine Tumors: Differential Diagnosis from Pancreatic Ductal Adenocarcinomas at MR Imaging-Retrospective Cross-sectional Study. *Radiology* 2017;284(1):77–87.
 67. Kawamoto S, Shi C, Hruban RH, et al. Small serotonin-producing neuroendocrine tumor of the pancreas associated with pancreatic duct obstruction. *AJR Am J Roentgenol* 2011;197(3):W482–W488.
 68. Kim MJ, Choi DW, Choi SH, Heo JS, Sung JY. Surgical treatment of solid pseudopapillary neoplasms of the pancreas and risk factors for malignancy. *Br J Surg* 2014;101(10):1266–1271.
 69. Law JK, Ahmed A, Singh VK, et al. A systematic review of solid-pseudopapillary neoplasms: are these rare lesions? *Pancreas* 2014;43(3):331–337.
 70. Gandhi D, Sharma P, Parashar K, et al. Solid pseudopapillary Tumor of the Pancreas: Radiological and surgical review. *Clin Imaging* 2020;67:101–107.
 71. Baek JH, Lee JM, Kim SH, et al. Small (≤ 3 cm) solid pseudopapillary tumors of the pancreas at multiphase multidetector CT. *Radiology* 2010;257(1):97–106.
 72. Yu MH, Lee JY, Kim MA, et al. MR imaging features of small solid pseudopapillary tumors: retrospective differentiation from other small solid pancreatic tumors. *AJR Am J Roentgenol* 2010;195(6):1324–1332.
 73. Tsitouridis I, Diamantopoulou A, Michaelides M, Arvanity M, Papaioannou S. Pancreatic metastases: CT and MRI findings. *Diagn Interv Radiol* 2010;16(1):45–51.
 74. Scatarige JC, Horton KM, Sheth S, Fishman EK. Pancreatic parenchymal metastases: observations on helical CT. *AJR Am J Roentgenol* 2001;176(3):695–699.
 75. Kim SH, Lee JM, Han JK, et al. Intrapancreatic accessory spleen: findings on MR Imaging, CT, US and scintigraphy, and the pathologic analysis. *Korean J Radiol* 2008;9(2):162–174.
 76. Sikka A, Adam SZ, Wood C, Hoff F, Harmath CB, Miller FH. Magnetic resonance imaging of pancreatic metastases from renal cell carcinoma. *Clin Imaging* 2015;39(6):945–953.
 77. Merkle EM, Bender GN, Brambs HJ. Imaging findings in pancreatic lymphoma: differential aspects. *AJR Am J Roentgenol* 2000;174(3):671–675.